ORIGINAL RESEARCH

Antagonism of the Thromboxane-Prostanoid Receptor as a Potential Therapy for Cardiomyopathy of Muscular Dystrophy

James D. West, PhD; Cristi L. Galindo, PhD, MBA; Kyungsoo Kim, PhD; John Jonghyun Shin, PhD; James B. Atkinson, MD, PhD; Ines Macias-Perez, PhD; Leo Pavliv, RPh; Bjorn C. Knollmann, MD, PhD; Jonathan H. Soslow, MD, MSCI; Larry W. Markham, MD, MSCR; Erica J. Carrier, PhD

***Background*—**Muscular dystrophy (MD) causes a progressive cardiomyopathy characterized by diffuse fibrosis, arrhythmia, heart failure, and early death. Activation of the thromboxane-prostanoid receptor (TPr) increases calcium transients in cardiomyocytes and is proarrhythmic and profibrotic. We hypothesized that TPr activation contributes to the cardiac phenotype of MD, and that TPr antagonism would improve cardiac fibrosis and function in preclinical models of MD.

***Methods and Results*—**Three different mouse models of MD (mdx/utrn double knockout, second generation mdx/mTR double knockout, and delta-sarcoglycan knockout) were given normal drinking water or water containing 25 mg/kg per day of the TPr antagonist ifetroban, beginning at weaning. After 6 months (10 weeks for mdx/utrn double knockout), mice were evaluated for cardiac and skeletal muscle function before euthanization. There was a 100% survival rate of ifetroban-treated mice to the predetermined end point, compared with 60%, 43%, and 90% for mdx/utrn double knockout, mdx/mTR double knockout, and delta-sarcoglycan knockout mice, respectively. TPr antagonism improved cardiac output in mdx/utrn double knockout and mdx/mTR mice, and normalized fractional shortening, ejection fraction, and other parameters in delta-sarcoglycan knockout mice. Cardiac fibrosis in delta-sarcoglycan knockout was reduced with TPr antagonism, which also normalized cardiac expression of claudin-5 and neuronal nitric oxide synthase proteins and multiple signature genes of Duchenne MD.

***Conclusions*—**TPr antagonism reduced cardiomyopathy and spontaneous death in mouse models of Duchenne and limb-girdle MD. Based on these studies, ifetroban and other TPr antagonists could be novel therapeutics for treatment of the cardiac phenotype in patients with MD. **(*J Am Heart Assoc*. 2019;8:e011902. DOI: 10.1161/JAHA.118.011902.)**

Key Words: Duchenne muscular dystrophy cardiomyopathy • receptor blocker • TC receptor

Muscular dystrophy (MD) is an umbrella term for a hereditary group of progressive neuromuscular diseases primarily distinguished by the specific dystrophin-glycoprotein complex proteins affected. Most predominant are the dystrophinopathies, Duchenne MD (DMD) and Becker MD, which are characterized by mutations in the X-linked dystrophin gene and affect ≈1:3500 live male births.[1] Overall, disruption of the dystrophin-glycoprotein complex results in mechanical instability of the myocyte membrane, pathological calcium influx via microtears, as well as channel activation, mitochondrial dysfunction, and protease-mediated necrosis.[2] Within cardiomyocytes, this process can lead to progressive dilated cardiomyopathy. As a result of advances in respiratory support, cardiomyopathy is now a primary cause of death among individuals with DMD and Becker MD,[3,4] while patients with the more heterogenous limb-girdle and Emery-Dreifuss MDs are also susceptible to cardiomyopathy, heart failure, and sudden death.[5]

Of the MDs, DMD cardiomyopathy is the most prevalent and consequently the best studied. The classic pathology of DMD is a subepicardial fibrosis in the posterobasal and left lateral wall of the left ventricle[6] that progresses to the remaining free wall, and finally to a diffuse myocardial fibrosis.[7,8] Fibrosis is usually well-established before functional decline is detected.[8]

From the Divisions of Allergy, Pulmonary, and Critical Care (J.D.W., E.J.C.), Cardiology (C.L.G., L.W.M.), and Clinical Pharmacology (K.K., B.C.K.), Division of Rheumatology and Immunology (J.J.S.), Department of Medicine, Department of Pathology, Microbiology, and Immunology (J.B.A.), and Division of Pediatric Cardiology, Department of Pediatrics (J.H.S.), Vanderbilt University Medical Center, Nashville, TN; Cumberland Pharmaceuticals Inc, Nashville, TN (I.M.-P., L.P.); Division of Pediatric Cardiology, Department of Pediatrics, Riley Hospital for Children and Indiana University School of Medicine, Indianapolis, IN (L.W.M.).

Accompanying Data S1, Table S1, and Figures S1 through S3 are available at https://www.ahajournals.org/doi/suppl/10.1161/JAHA.118.011902

Correspondence to: Erica J. Carrier, PhD, Division of Allergy, Pulmonary, and Critical Care, Vanderbilt University Medical Center, P475G MRB IV, 2213 Garland Avenue, Nashville, TN 37232. Email: erica.carrier@vumc.org

Received December 28, 2018; accepted September 23, 2019.

Clinical Perspective

What Is New?

- This is the first report demonstrating that oral administration of a thromboxane-prostanoid receptor antagonist improves survival and cardiomyopathy in multiple mouse models of Duchenne and limb-girdle muscular dystrophy, with little effect on skeletal muscle.
- This efficacy of antagonism suggests that endogenous thromboxane-prostanoid receptor activation contributes to the cardiac phenotype of muscular dystrophy.

What Are the Clinical Implications?

- Antagonism of the thromboxane-prostanoid receptor has the therapeutic potential to ameliorate or delay the cardiomyopathy of muscular dystrophy, which could extend patient lifespan.
- Because these effects occur downstream of dystrophin expression and regardless of pathogenesis, antagonist treatment could be either first-line or adjunct to gene replacement therapy.

Although manifestation of clinical heart failure may be delayed in wheelchair-bound patients, cardiomyopathy proceeds to systolic dysfunction and heart failure symptoms in DMD by the second or third decade of life, followed by inevitable and early death. Arrhythmias, with potential for sudden cardiac death, are also common in individuals with MD, and their risk correlates with the fibrosis seen through imaging or autopsy,[7,9] even with minimal decrease in cardiac function.[10] Thus, there is an urgent need for MD therapies to both support cardiac function and prevent fibrosis.

The G protein–coupled thromboxane-prostanoid receptor (TPr), expressed in platelets, immune cells, smooth muscle, and cardiomyocytes, has deleterious consequences of activation in the heart that mirrors the fibrosis and calcium alterations associated with MD cardiomyopathy. TPr activation contributes to left ventricular (LV) hypertrophy and heart failure in mouse models of systemic hypertension and Gh overexpression.[11–13] Activation of the TPr is profibrotic in multiple systems,[14,15] and we have shown that TPr antagonism dramatically decreases right ventricular fibrosis and improves cardiac function in a pressure-overload model of pulmonary arterial hypertension.[16] The best-characterized signaling pathway of the TPr is via Gq,[17] resulting in phospholipase C activation, calcium mobilization via intracellular stores, and protein kinase C activation. In ventricular cardiomyocytes, TPr activation causes increased intracellular calcium, arrhythmia, and cell death in ventricular cardiomyocytes,[18] and administration of a TPr agonist induces ventricular arrhythmias in rabbits.[19]

Furthermore, available TPr is likely to be activated during MD. One endogenous TPr ligand, 15-F_{2t}-isoprostane, formed during oxidative stress and known to cause fibrosis through the receptor,[14] is increased 4-fold in patients with Becker MD and those with DMD,[20] as well as in individuals with class IV heart failure from other causes.[21] We thus postulated that ligand availability and known signaling actions position this receptor to impact cardiomyopathy and the decline of cardiac function in MD, where it may be an important therapeutic target. To test this hypothesis, we used the specific TPr antagonist ifetroban to block receptor activity in several mouse models of MD that use multiple mechanisms of disease to recapitulate different aspects of the human cardiac phenotype.

Methods

The authors declare that all data are available within the article and supplementary files, and methods and materials used to conduct the research herein will be made available to any researcher upon reasonable request for purposes of reproducing the results.

Experimental Protocols

This study was performed in accordance with the National Institutes of Health's Public Health Service Policy of Humane Care and Use of Laboratory Animals and the Animal Welfare Act. All protocols were approved by the Vanderbilt University Institutional Animal Care and Use Committee. Experiments were performed using appropriate anesthetics and analgesics, and every effort was made to minimize animal pain and distress. The minimum amount of isoflurane required for animal sedation was used. Animal weight was monitored each week, and mice demonstrating weight loss or lethargy were given saline, as well as supplementary nutrition and water in an accessible, ground-level dish, and closely monitored. This was not a survival experiment by design, and experiments with mdx/utrn and second-generation mdx/mTR knockout (KO) mice were halted after excessive mortality in vehicle-treated mice.

Experimental Animal Models

Three mouse models of MD were used for these experiments. The first were mice null for both dystrophin and utrophin (mdx/utrn$^{(-/-)}$; double KO [DKO]), bred from commercially available mdx mice that are haploinsufficient for utrophin (*Utrn*^{tm1Ked}/*Dmd*^{mdx}/J, Jackson #014563).[22] The second were mice null for both dystrophin and telomerase RNA component (mdx/mTR KO; B6.Cg-*Terc*^{tm1Rdp}/*Dmd*$^{mdx-4Cv}$/BlauJ, Jackson #023535).[23] These mice have shortened telomeres similar to human patients with DMD,[24] and their phenotype becomes

successively worse over generations. Second-generation mice, bred from first-generation pairs of mdx/mTR KO, were used for experiments. Both sets of mice were genotyped according to Jackson protocol. The third model included δ-sarcoglycan (dSG) KO mice,[25] generously donated as heterozygous pairs by Dr Kevin Campbell at the University of Iowa. These were directly bred as homozygous dSG KO. The dSG and mdx/mTR mice were on the C57BL/6 background, and wildtype (WT) mice were C57BL/6 strain, derived from the original dSG heterozygous pairs and bred in-house. Age-matched C57BL/6 mice were also used as a reference for the DKO mice (which were C57BL/10ScSn background) although the primary evaluation was between vehicle- and drug-treated DKO. A detailed comparison of the significant phenotypic difference between DKO and the WT C57BL/10 or C57BL/10ScSn strains as well as mdx littermates can be found elsewhere.[22,26,27]

Randomization and Drug Treatment

All mice were randomly assigned at weaning, 3 weeks of age, to receive either vehicle (normal drinking water) or water containing the TPr antagonist ifetroban. Obvious runts were excluded. Randomization was directed by a person blinded to everything but weanling number and sex, and group numbers were balanced as well as possible throughout the study. Randomization occurred on a sex and cage basis per litter (eg, females from 1 litter were assigned to vehicle and the males to drug, while the next litter may have males assigned to vehicle and females to drug). Care was taken to ensure that litters from different breeder pairs were randomized to both groups. In the case of DKO mice, weanling cages were randomized before genotyping, and mdx/utrn$^{(-/+)}$ and mdx/utrn$^{(+/+)}$ mice were later removed from the study. This contributed to the overall randomization. WT mice were assigned to either 10-week (DKO) or 6-month (mdx/mTR and dSG KO) studies. From an initial sample size calculation, the initial goal was 10 WT and 20 MD mice per treatment group, divided equally between the sexes; however, this was expanded to 15 mice/sex/group in dSG KO mice once sex differences in phenotype were observed.

The TPr antagonist ifetroban (Cumberland Pharmaceuticals) was added directly to an external bottle, the only source of drinking water, at a concentration that yielded a 25-mg/kg per day dose.[16] Mice were weighed and dose/water was changed once a week. Vehicle-treated mice received standard water from a central supply.

Experimental Design

Mice began treatment with either vehicle or drug at weaning (3 weeks) and continued for the predetermined duration of the study, chosen based on published life expectancy. mdx/mTR and dSG KO mice were euthanized at 6 months of age, while DKO mice were euthanized at 10 weeks. Any spontaneous deaths were noted. Mice were evaluated for spontaneous running on wireless in-cage running wheels 12 days before euthanization, followed by functional testing by wire hang, and echocardiography 1 day before euthanization. mdx/mTR and dSG KO mice had an additional midpoint evaluation at 3 months, consisting of spontaneous running, wire hang, echocardiography, and blood draw via submandibular puncture. At euthanization, mice were anesthetized and underwent pressure-volume catheterization of the left ventricle or blood draw from the jugular for cardiac troponin analysis, followed by euthanization. Total body weight and heart weight were measured and compared with tibial length to compensate for any additional weight caused by muscle pseudohypertrophy or fluid retention.

Functional Testing

Spontaneous running was tested using low-profile in-cage wireless running wheels (Med-Associates, Inc) and revolutions were translated to kilometers in the manufacturer's Wheel Manager software. Mice were transferred to single housing and given 3 days to acclimate to running wheels, and recordings were then taken for 7 days. Based on preliminary studies with WT mice, the final 4 days were averaged to determine the distance run per day. Limb strength was also measured by wire hang, according to the Longest Suspension Time Method in Treat-NMD SOP DMD_M.2.1.004.[28]

Echocardiography

Transthoracic 2-dimensional echocardiography in B mode, pulsed-wave Doppler, and M mode was performed in isoflurane-anesthetized mice using a Vevo 770 (VisualSonics) with a small animal transducer, as previously described.[29] To avoid a confounding influence of inhaled isoflurane on cardiovascular function, echocardiographic data were excluded from any mouse that reacted unduly to anesthesia (mean heart rate <300 beats per minute).

Pressure-Volume Catheterization

Mice were given tribromoethanol (Avertin) intraperitoneally to induce a surgical plane of anesthesia and shaved to expose the abdomen and chest. Animals were ventilated with isoflurane via endotracheal intubation before opening of the thorax for open-chested catheterization. Through the diaphragm, a needle stab incision was made in the left ventricle and a 1.4F (0.4 mm diameter) dual electrode Millar

micromanometer/volume catheter (ADInstruments) advanced into the left ventricle through the needle hole. Pressure-volume signals were recorded using PowerLab for LabChart Pro (ADInstuments). Mice were euthanized and blood and tissue were collected while still under surgical plane of anesthesia. Catheterization was attempted on DKO mice but intubation failed as a result of their extreme kyphosis.

Histology

Upon dissection, heart and tibialis anterior (TA) were snap-frozen in optimal cutting temperature. Ten micrometer transverse sections of hearts were sliced and stained with Masson trichrome for visualization of fibrosis according to the Treat-NMD SOP MDC1A_M.1.2.003.[30] The TA and diaphragm were evaluated for fibrosis as previously described,[29] averaging 4 fields per mouse from multiple slices. TA necrosis was quantified in DKO mice using ImageJ, where photos of trichrome stain were converted to greyscale by separating color channels. The green channel was thresholded to a dark background, highlighting lightly stained necrotic cells and extracellular volume, and the automatic threshold was used to calculate area fraction for each photo. A total of 4 fields per mouse were averaged. Cardiac slides were scanned at 20× using the Leica SCN400 slide scanner and evaluated for fibrosis in the Leica Tissue IA Optimizer using a constant defined mask. In each case, the total number reflects all acceptable slides available.

Cardiomyocyte Contraction and Calcium Handling

Ventricular cardiomyocytes were isolated via Langendorff perfusion in the presence of the ATPase inhibitor butanedione monoxime, and then transferred to a butanedione monoxime–free extracellular solution. Single-cell contractility was measured following a 1-Hz field stimulation. Cardiomyocytes were then loaded with Fura-2 and calcium flux measured from healthy cells after transient stimulation with 1 Hz or 10 mmol/L caffeine spritz.[31,32]

Molecular Studies

RNA and protein were isolated from the apical portion of the left ventricle using RNeasy (Qiagen) and radioimmunoprecipitation assay buffer with protease inhibitors. The following antibodies were used for immunoblotting: claudin-5 (#ABT45, Millipore), neuronal nitric oxide synthase (nNOS) (#4234S, Cell Signaling), HSP70 (Enzo Life Sciences), and phospho- and total SMAD2/3 (Cell Signaling).

RNAseq

LV mRNA was pooled from multiple mice per sample, where number of dSG samples was only determined by RNA quality (n=2 per group except ifetroban-treated dSG KO n=3), and RNAseq performed on an Illumina HiSeq3000 system by VANTAGE (Vanderbilt Technologies for Advanced Genomics). A complete description of sample preparation and data analysis is available in Data S1. Raw reads (fastq files) were analyzed via the Partek flow server and Partek Genomics Suite 6.6, with statistical comparison of groups performed using Partek best fit multimodel algorithm (gene-specific analysis). Genes with a $P<0.05$ by Benjamini & Hochberg multiple hypothesis testing were considered significantly altered. Statistical analyses for identification of overrepresented ontologies, functions, and pathways were performed using DAVID, a freely available online-based functional analysis tool (http://david.abcc.ncifcrf.gov), after initial statistical data analysis identified relevant gene sets. Ingenuity (Qiagen) was used for functional grouping and predictive modeling, and Gene Set Enrichment Analysis (Broad Institute) was used to evaluate biological process enrichment and identify activation of transcription factors.

Data Handling and Statistical Analysis

The mdx/mTR and dSG KO mice shared 6-month WT groups. Data analysis, excluding RNAseq, was performed in Prism (GraphPad) to determine statistical significance. Comparisons were primarily made between vehicle- and drug-treated MD groups, by 2-tailed *t* test, or groups were compared with WT by 1-way or 2-way ANOVA followed by Holm-Sidak posttest; Mann–Whitney or Kruskal–Wallis with Dunn posttest were used to analyze nonparametric data, ascertained by a D'Agostino and Pearson normality test. Survival curves were compared by Mantel-Cox log-rank test. Values are expressed as mean±SEM, and sample size given for each figure.

Results

To determine whether TPr antagonism improves the cardiac phenotype of DMD, we treated mdx/utrn$^{(-/-)}$ DKO mice, a model of severe DMD, with the TPr antagonist ifetroban from 3 to 10 weeks of age. TPr antagonism improved survival to 10 weeks from 60% in vehicle-treated to 100% in ifetroban-treated animals (Figure 1A) and increased stroke volume and cardiac index (cardiac output normalized to weight; Figure 1B) compared with vehicle-treated surviving mice. DKO heart weight, both alone and normalized to tibial length, did not differ with ifetroban treatment (5.00±0.57 g/mm for vehicle and 4.93±0.51 g/mm with ifetroban). Similarly, in second-generation mdx/mTR$^{(-/-)}$ mice, a model of DMD with

shortened telomeres,[23] treatment with ifetroban improved 6-month survival from 43% to 100%, and increased the 3-month cardiac index, primarily as a result of increased stroke volume (Figure 1C and 1D).

While the 10-week-old DKO mice had profound fibrosis of the diaphragm and fibrosis/necrosis of the TA, which did not improve with TPr antagonism (Figure 2A and 2B), they did not yet display the diffuse myocardial fibrosis characteristic of DMD (Figure 2C). Furthermore, the severe kyphosis in both DKO treatment groups prevented intubation for invasive hemodynamics, while the high spontaneous mortality of DKO and mdx/mTR mice precluded tissue collection and made survivor bias likely. Therefore, to more completely examine the effects of TPr antagonism on the MD cardiac phenotype, we used dSG KO mice, which contain a mutation associated with limb-girdle MD type 2F and develop a dilated cardiomyopathy with diffuse fibrosis, similar to individuals with other forms of MD.[25] dSG KO mice had overall better 6-month survival (90%) compared with the other genotypes used, which improved to 100% with ifetroban treatment (Figure 3A). Noticeably, the few deaths in dSG KO mice occurred either during or just following placement of in-cage running wheels

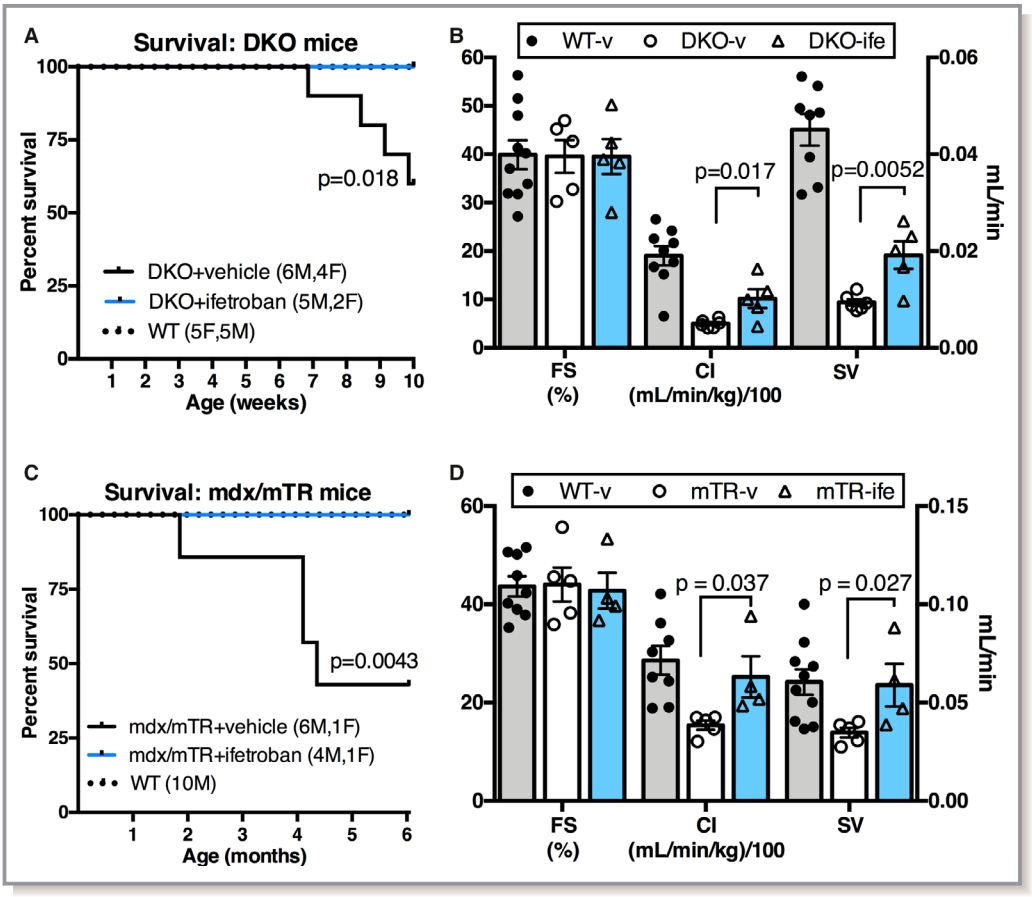

Figure 1. Thromboxane-prostanoid receptor (TPr) antagonism increased survival and cardiac output in 2 Duchenne muscular dystrophy (DMD) mouse models. **A**, Survival of double knockout (DKO) mice to the predetermined 10-week time point. Curves were compared by Mantel Cox log-rank test, and number/sex of mice in each group are shown. Six DKO mice, including both vehicle- and ifetroban-treated mice, were accidentally placed on high-fat breeder chow for several weeks that led to improved weight gain and health compared with previous generations; these mice were omitted from survival analysis. **B**, Echocardiography analysis of the DKO cohort. n=10 wildtype (WT) and 5 to 6 as shown per DKO group (left ventricular measurements could not be obtained for 1 vehicle-treated mouse). The mean and standard error of each measurement are shown, and comparisons between vehicle-treated and ifetroban-treated DKO were made by 2-tailed *t* test. **C**, Survival and (**D**) echocardiography of male mdx/mTR mice. Because so few vehicle-treated mice survived to 6 months, echocardiographs are from 3 months of age; echocardiographs from 3-month-old WT male mice are shown for comparison. n=8 to 10 WT, n=5 vehicle-treated, and n=4 ifetroban-treated mdx/mTR. Statistical analysis of groups was performed as in (**A** and **B**). CI indicates cardiac index (cardiac output normalized to body surface area); FS, fractional shortening; SV, stroke volume.

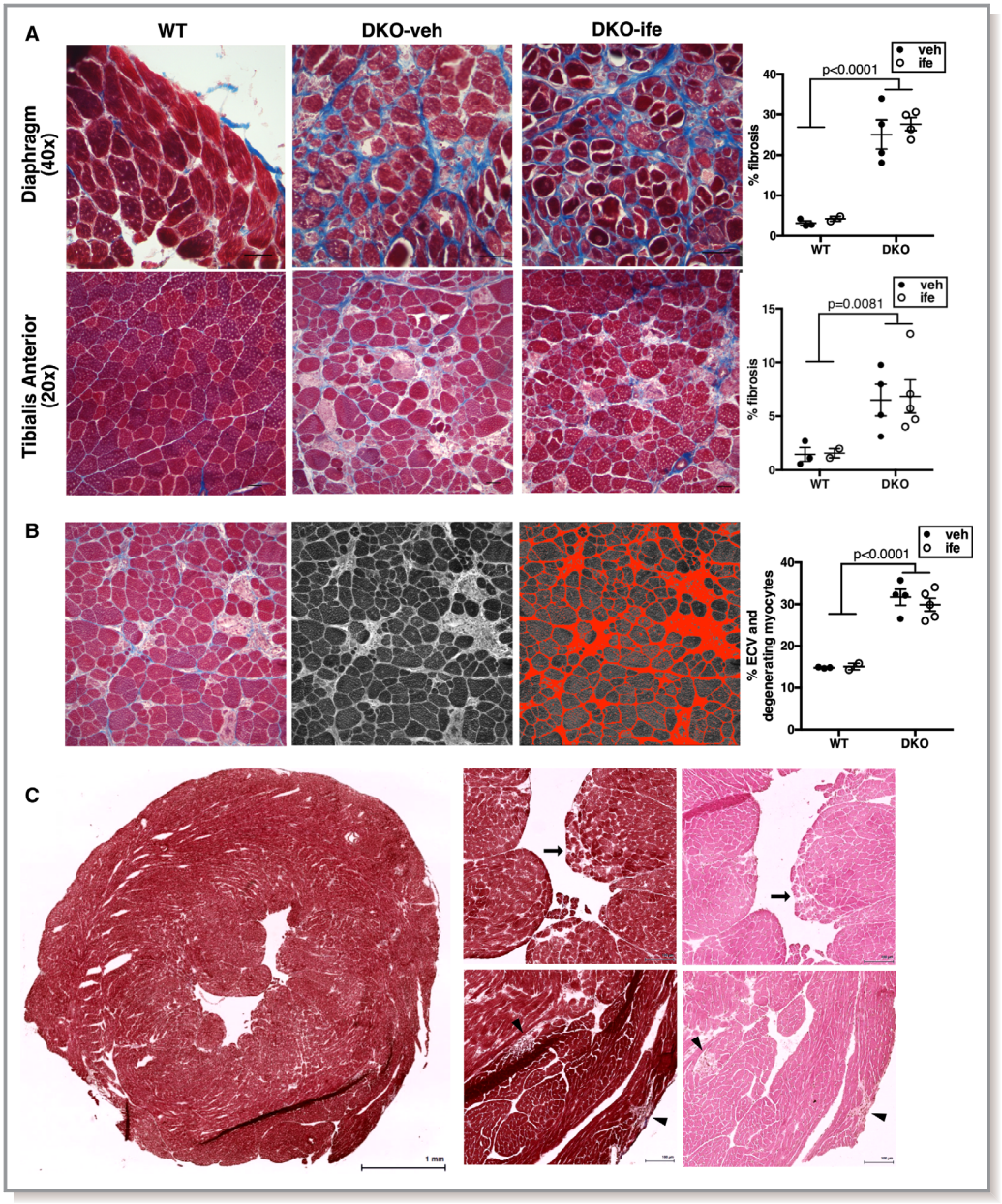

Figure 2. Double knockout (DKO) histology. **A**, Thromboxane-prostanoid receptor (TPr) antagonism does not improve skeletal muscle fibrosis. Shown is diaphragm (top) at 40× and tibialis anterior (TA, bottom) at 20×, stained with Masson trichrome. Scale bar=50 μm. Fibrosis (blue) was quantitated in NIS elements and averaged from 4 fields per mouse. Groups were compared using 2-way ANOVA/Holm-Sidak. The mean and standard error is shown. **B**, TPr antagonism does not prevent skeletal muscle degeneration. Degenerating myocytes stain lighter than intact cells with Masson trichrome.[30] This, along with the increased extracellular volume (ECV) as a result of interstitial fibrosis, was quantified after separation of color channels in ImageJ. Shown is the original 20× photo of DKO TA (left), the green color channel (middle), and the automatically thresholded light area (right). Four fields per mouse were averaged, with the mean and standard error of 2 to 5 mice per group as shown. Groups were compared using 2-way ANOVA/Holm-Sidak. **C**, DKO hearts demonstrate little fibrosis at 10 weeks. Shown is a whole heart slice from a vehicle-treated DKO mouse at approximately ×1.4 magnification (scale bar=1 mm), and selected areas at ×10 magnification (scale bar=100 μm). At left is the trichrome stain, where collagen appears blue, and at right is the region stained with hematoxylin and eosin. Unlike skeletal muscle, discrete patches of necrosis in the heart (arrowheads) were characterized by cellular infiltration. Cardiomyocyte disorganization and size variability can be seen in the middle panels (arrows).

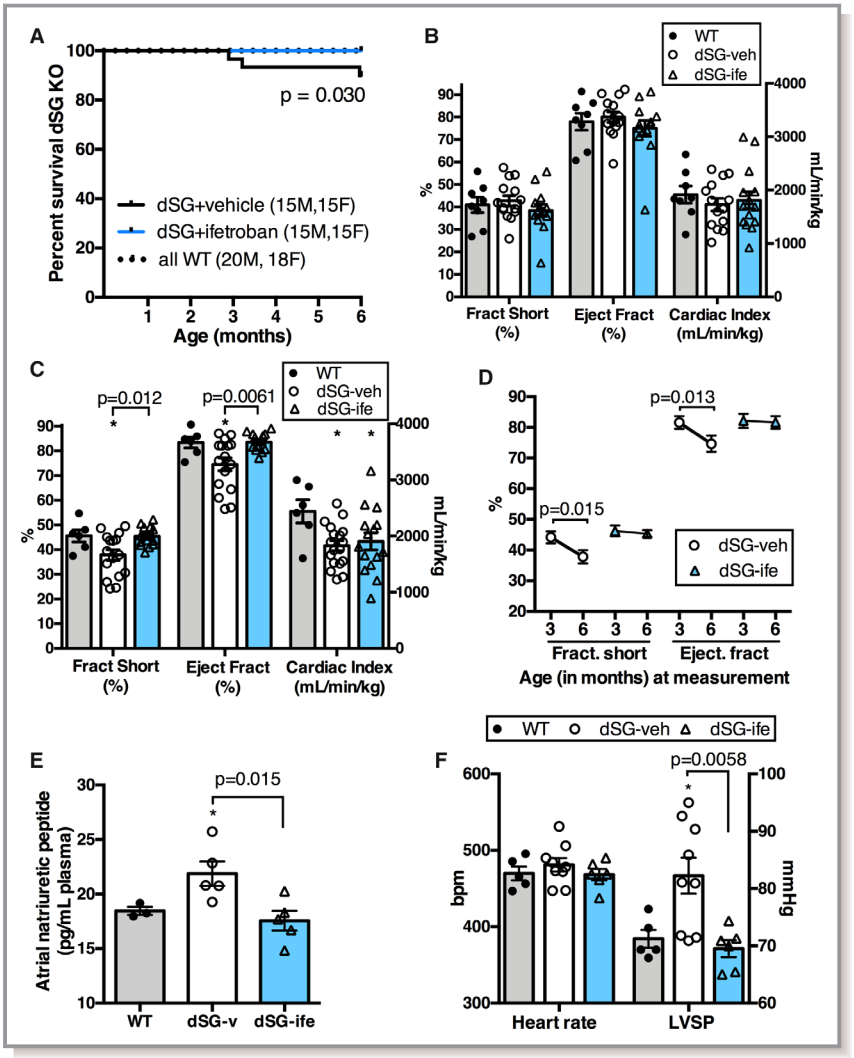

Figure 3. Antagonism of the thromboxane-prostanoid receptor (TPr) improves cardiomyopathy in δ-sarcoglycan (dSG) knockout (KO) male mice. **A**, Survival of dSG mice to the 6-month end point, compared with wildtype (WT). Curves were compared by Mantel Cox log-rank test, and number of mice in each group are shown. **B**, Echocardiography of 6-month-old female mice. There were no significant differences between either KO group and WT by 1-way ANOVA, or between vehicle- and drug-treated KO by 2-tailed *t* test. **C**, Echocardiography of 6-month-old male mice. Vehicle- and drug-treated dSG KO were compared by 2-tailed *t* test, and KO compared with WT by 1-way ANOVA/Holm-Sidak (**P*<0.05). n=6 to 7 WT, n=15 dSG-vehicle (dSG-veh), and n=13 dSG-ifetroban (dSG-ife). **D**, Longitudinal comparison of fractional shortening and ejection fraction, from 3- and 6-month male echocardiographs; TPr antagonism prevents the decline in cardiac function seen in dSG KO mice. n=15 dSG-veh and n=13 dSG-ife; 3-month echocardiographs were compared with 6-month echocardiographs by 2-tailed paired *t* test within each group. The change from 3 to 6 months is shown for each group, along with the mean and standard error of echocardiographic values. **E**, Plasma atrial natriuretic peptide in 6-month-old mice, determined by ELISA. n=3 WT, 5 for each dSG KO; vehicle- and drug-treated dSG KO were compared by 2-tailed *t* test, and KO compared with WT by 1-way ANOVA/Holm-Sidak (**P*<0.05). **F**, Left ventricular systolic pressure (LVSP) is elevated in dSG-KO male mice, but the increase in pressure is prevented with TPr antagonism. Shown are the mean and standard error from pressure-volume catheterization of male mice, performed at 6 months just before euthanization. Groups were compared by *t* test and 1-way ANOVA/Holm-Sidak posttest as previously described (**P*<0.05). Bars in (**B**, **C**, **E**, and **F**) indicate mean and standard error of group data. ANP indicates atrial natriuretic peptide.

before 3- and 6-month echocardiographs (Figure 3A); this corresponds with initial reports of sudden cardiac death in these mice following forced treadmill exercise.[25] At 6 months, heart weights and ratios were not significantly increased from WT, although dSG KO mice exhibited pseudohypertrophy of hind leg muscles, similar to patients with DMD, which led to an elevated body weight (Table). Physical parameters of dSG KO, DKO, and mdx/mTR mice are summarized in the Table.

Cardiac parameters of female dSG KO mice did not differ significantly from WT mice (Figure 3B), and decreased functional impairment and cardiac fibrosis in female versus male dSG KO mice has recently been reported.[33] Therefore, we confined our analyses to male mice. Male dSG KO mice exhibited a decline in ejection fraction and fractional shortening, which was prevented with ifetroban treatment (Figure 3C and 3D). Cardiac index was slightly decreased in both groups of dSG KO (Figure 3C), but this may have been secondary to the increased weights of the dSG KO, as cardiac output was not significantly decreased (Figure S1). Coinciding with the normal heart weights, via echocardiography the dSG KO decline in ejection fraction was not accompanied by dilation but did correspond with increased plasma atrial natriuretic peptide, which was also normalized with TPr antagonism (Figure 3E). Plasma brain natriuretic peptide and

Table. Animal Physical Data

	Treatment	Body Weight, g	Body Weight: Tibial Ratio, g/mm	Heart Weight, mg	Heart:Tibial Ratio, mg/mm	No.
Group: 10 wk						
WT males	Vehicle	27.08±1.91	5.43±0.77	156.6±24.9	8.28±1.42	5
	Ifetroban	29.80±1.10 *P*=0.046	4.76±0.26 *P*=0.038	142.0±11.9	7.87±0.65	5
DKO males	Vehicle	18.53±3.32 *P*<0.0001	4.44±0.40 *P*=0.012	81.5±11.3 *P*<0.0001	4.84±0.59 *P*<0.0001	4
	Ifetroban	19.10±1.21 *P*<0.0001	4.31±0.15 *P*=0.0052	82.6±8.1 *P*<0.0001	4.97±0.49 *P*<0.0001	5
WT females	Vehicle	20.62±2.40	5.80±0.33	119.2±9.9	6.73±0.42	5
	Ifetroban	23.95±0.21	5.72±0.13	137.0±4.2 *P*=0.069	7.56±0.15 *P*=0.082	2
DKO females	Vehicle	20.73±1.29	4.28±0.45 *P*=0.0008	88.7±9.9 *P*=0.0068	5.23±0.56 *P*=0.0061	3
	Ifetroban	16.95±4.17	4.60±0.26 *P*=0.0056	77.5±14.8 *P*=0.0036	4.83±0.77 *P*=0.0050	2
Group: 6 mo						
WT males	Vehicle	28.72±3.11	1.65±0.13	150.2±18.3	8.39±1.01	10
	Ifetroban	29.58±1.88	1.64±0.11	144.9±11.6	8.01±0.70	10
mdx/mTR males	Vehicle	30.95±1.55	1.69±0.08	145.0±5.7	7.90±0.12	2
	Ifetroban	28.98±2.08	1.59±0.20	142.3±19.3	7.81±0.97	4
dSG KO males	Vehicle	33.38±2.25 *P*=0.0010	1.82±0.13 *P*=0.0047	160.7±20.1	8.78±1.17	13
	Ifetroban	31.85±2.22 *P*=0.029	1.76±0.10 *P*=0.085	145.2±21.1	8.02±1.17	14
WT females	Vehicle	24.75±0.81	1.37±0.04	126.5±14.0	6.98±0.74	8
	Ifetroban	23.20±1.05 *P*=0.084	1.29±0.06 *P*=0.044	118.7±10.9	6.61±0.59	10
dSG KO females	Vehicle	26.72±2.04 *P*=0.037	1.49±0.09 *P*=0.0034	121.2±9.6	6.74±0.44	14
	Ifetroban	26.29±1.96 *P*=0.084	1.46±0.09 *P*=0.015	120.4±9.7	6.70±0.49	15

Mean±SD of parameters taken at euthanization or necropsy (from 1 double knockout [DKO] female that died on day 69). Six DKO mice accidentally placed on high fat breeder chow were excluded. *P* values of the differences from wildtype (WT) by 1-way ANOVA/Holm-Sidak are shown when significant ($P<0.05$) or approaching significance. No ifetroban-treated KO groups were significantly different from vehicle-treated KO by unpaired 2-tailed *t* test. dSG indicates δ-sarcoglycan.

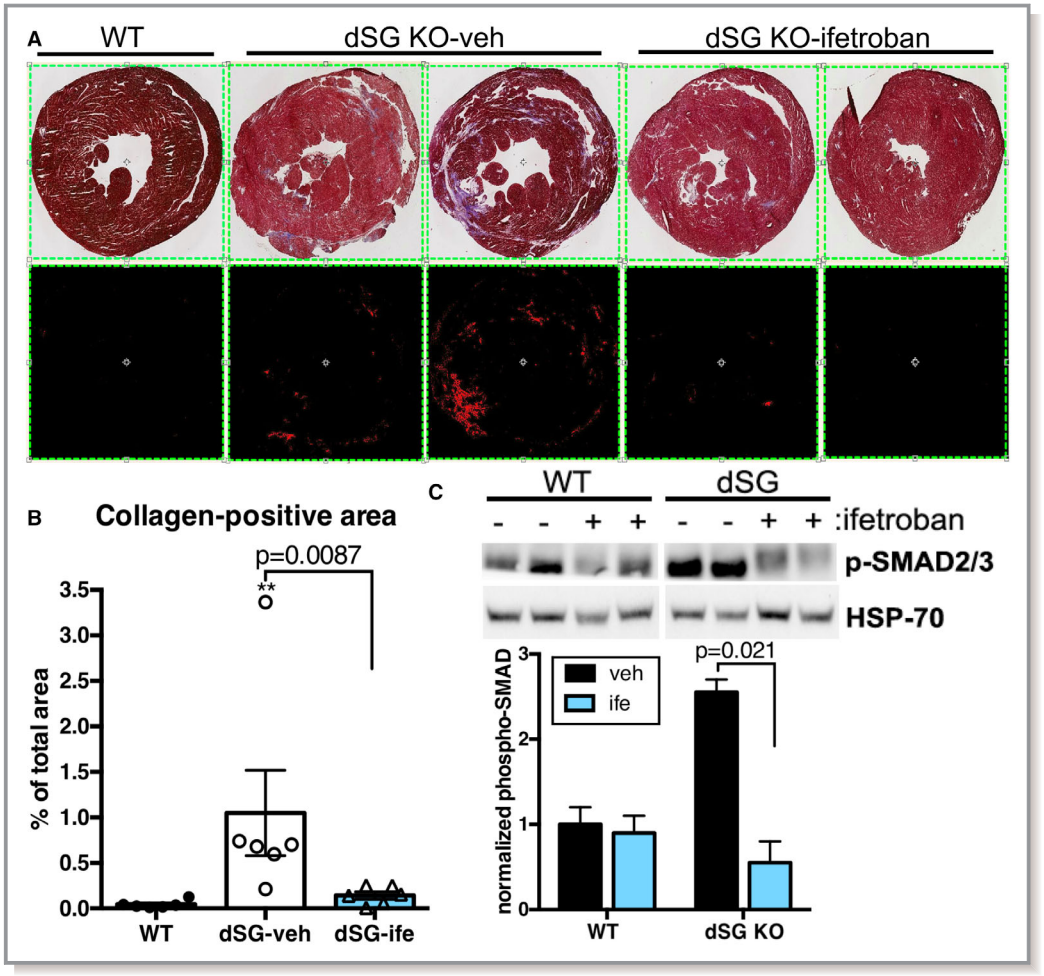

Figure 4. Thromboxane-prostanoid receptor antagonism prevents development of cardiac fibrosis in δ-sarcoglycan (dSG) knockout (KO) mice. **A**, At top are representative whole heart slices from wildtype (WT) and dSG KO male mice, stained with trichrome, and below are the image masks used to quantify the blue stain of fibrosis. **B**, Results of fibrosis stain quantification, normalized to total area. The mean and standard error are shown. Drug-treated male dSG KO were compared with vehicle-treated KO by Mann–Whitney test; both groups were compared with WT by Kruskal–Wallis (**P=0.0013; P=0.39 for dSG-ifetroban vs WT). **C**, As previously shown,[16] ifetroban treatment reduced SMAD2/3 phosphorylation, a canonical marker of transforming growth factor-β activity. Band density of phospho-SMAD2/3 was quantified in ImageJ and normalized to HSP70 (heat shock protein 70); gap indicates missing lanes. Vehicle-treated dSG KO was compared with drug-treated males by 2-tailed t test; the mean and standard error of n=2 are shown.

cardiac troponin analysis in dSG KO mice did not significantly differ from WT (data not shown). In addition to cardiac decline, male dSG KO mice also had elevated LV systolic pressure, which was normalized with TPr antagonism (Figure 3F).

dSG KO cardiomyopathy was accompanied by increased myocardial fibrosis, particularly in the epicardial LV free wall. Treatment with the TPr antagonist decreased myocardial fibrosis in dSG mice (Figure 4A and 4B), and similarly decreased SMAD2/3 phosphorylation, a key mediator of profibrotic transforming growth factor-β signaling (Figure 4C). Similar to the DKO, there was no difference in TA fibrosis with treatment (Figure 5A), nor an effect on spontaneous running or grip hang in either males or females (Figure 5B and 5C). This suggests that TPr antagonism selectively preserves cardiac but not skeletal muscle function in MD.

To determine whether TPr antagonism affected the contractile properties of cardiomyocytes at 6 months, we measured contraction of isolated cardiomyocytes following a train of field stimulation (1 Hz for 20 seconds). dSG KO cardiomyocytes demonstrated ≈20% less sarcomeric shortening compared with WT, which was not improved in cardiomyocytes from ifetroban-treated mice (Figure 6A), although initial sarcomere length was the same (data not shown). However, vehicle-treated, but not ifetroban-treated, dSG KO cardiomyocytes had impaired sarcomeric relaxation (Figure 6B). When loaded with Fura-2 AM, dSG KO cardiomyocytes had normal diastolic levels

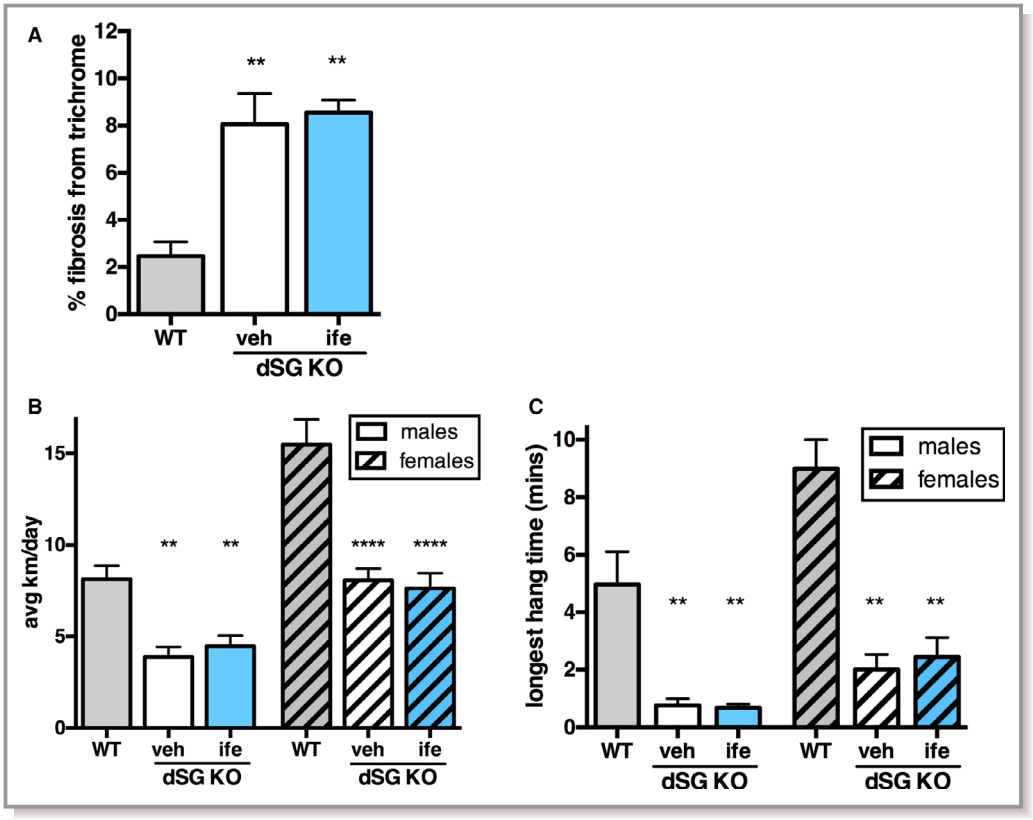

Figure 5. Treatment with thromboxane-prostanoid receptor (TPr) antagonist did not affect δ-sarcoglycan (dSG) knockout (KO) skeletal muscle fibrosis or function. **A**, Ifetroban did not decrease fibrosis of TA muscles in 6-month-old male mice. Shown are the mean and standard error of trichrome stain as a fraction of the total area at 10×, 4 representative fields per slice (n=4–5). ***P*=0.0026 vs wildtype (WT) by 1-way ANOVA; drug and vehicle-treated KO were compared by 2-tailed *t* test. Similarly, TPr antagonism did not affect spontaneous running on in-cage running wheels (**B**), and longest hang in 3 trials of the wire hang (**C**; max hang 10 minutes as per protocol) at 6 months in male and female mice, with mean and standard error (n=10–14). Ifetroban treatment had no significant effect on any dSG KO group. ***P*<0.01 and *****P*<0.0001 vs WT by 1-way ANOVA followed by Holm–Sidak or Kruskal–Wallis test with Dunn multiple comparison (wire hang). The results of comparisons between drug- and vehicle-treated KO by 2-tailed *t* test or 2-tailed Mann–Whitney *t* test (wire hang) were not significant (*P*=0.72 in **A**, *P*=0.47 for males and 0.71 for females in **B**, and *P*=0.77 for males and 0.58 for females in **C**).

of intracellular calcium (Ca^{2+}; Figure 6C). Mirroring the contraction data, cardiomyocytes from both dSG KO groups tended toward decreased amplitude of stimulated Ca^{2+} release (Figure 6D), while vehicle-treated dSG KO cardiomyocytes demonstrated elongated Ca^{2+} transient decay (tau) that was ameliorated in cardiomyocytes from ifetroban-treated mice (Figure 6E). This was independent of SERCA2 expression or phospholamban phosphorylation (Figure S2A); as no exogenous ifetroban was added to the experimental buffer, this suggests that the delayed Ca^{2+} clearance and relaxation is caused by cellular remodeling, prevented by TPr antagonism. Caffeine-stimulated Ca^{2+} removal (reflective of NCX transport) was similarly faster in both ifetroban- and vehicle-treated dSG KO cardiomyocytes (Figure 6F).

Because TPr antagonism in dSG KO mice improved cardiomyocyte and whole heart remodeling and function without directly affecting myocyte contraction, we examined expression of several proteins that contribute to cardiomyopathy in MD. nNOS expression is reduced in cardiac and skeletal muscle of patients and mice with DMD,[34,35] and its restoration prevents cardiomyopathy in animal models of MD.[35–37] Protein levels of nNOS were reduced in dSG KO mouse hearts, but not in hearts of dSG KO mice given ifetroban (Figure 7A). Similarly, expression of the tight junctional protein claudin-5 is decreased in DKO and dSG KO mice,[38,39] as well as in end-stage human cardiomyopathy,[40] while its replacement prevents myocardial dysfunction in dSG KO and DKO mice.[38,41] The decrease of claudin-5 expression in the dSG KO heart was also normalized with TPr antagonism (Figure 7B).

To identify molecular mechanisms that might underlie our phenotypic observations in dSG KO hearts following ifetroban

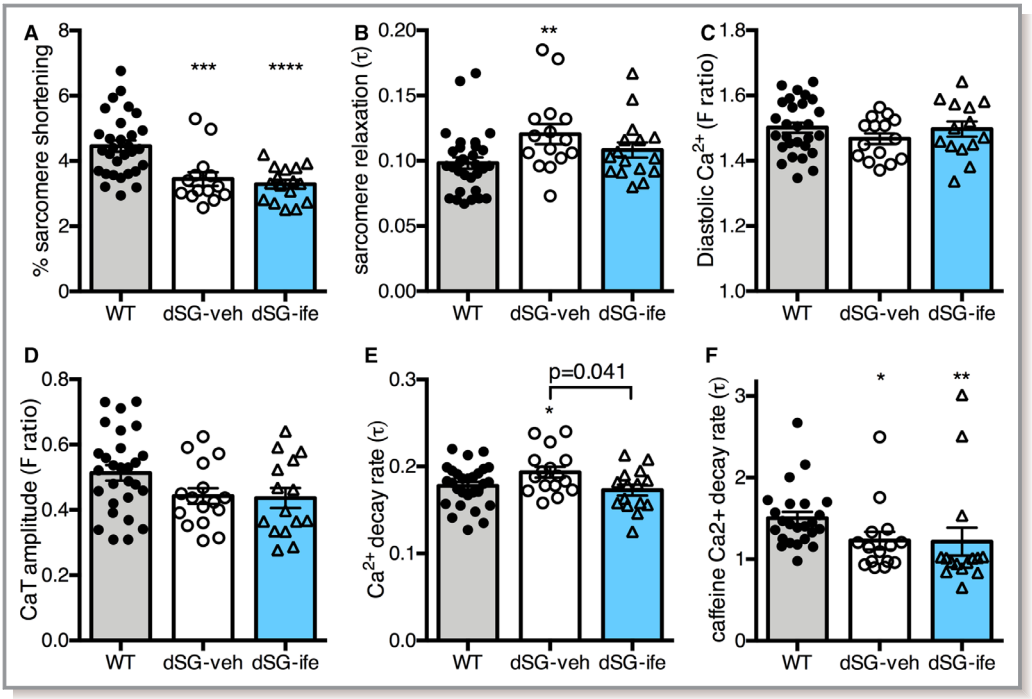

Figure 6. Cardiomyocytes from mice given thromboxane-prostanoid receptor antagonist still have contraction deficits, but the delayed relaxation is ameliorated. **A**, Cardiomyocyte contraction following a 1-Hz field stimulus, and (**B**) the decay rate of relaxation, demonstrating delayed relaxation in cardiomyocytes from vehicle-treated but not ifetroban-treated male δ-sarcoglycan (dSG) knockout (KO) mice. **C**, Resting (end-diastolic) Ca^{2+} after loading with Fura-2, which was not elevated in dSG KO mice. **D**, Amplitude of Ca^{2+} transients following stimulation with 1 Hz, and (**E**) the decay rate of Ca^{2+} transients; similar to contraction measurements, delayed clearance was seen in vehicle-treated dSG KO cardiomyocytes. However, the decay of calcium released from the sarcoplasmic reticulum following a 10-mmol/L caffeine spritz (**F**), which reflects NCX activity, was faster in cardiomyocytes from both vehicle-treated and drug-treated dSG KO mice. Shown are the means and standard errors of values; n=30 wildtype (WT) cardiomyocytes and 16 each dSG KO. Groups were compared by 1-way ANOVA and Holm-Sidak posttest, except (**B** and **F**), which were compared with Kruskal–Wallis and Dunn posttest; **P*<0.05, ***P*<0.01, ****P*<0.001, and *****P*<0.0001 vs WT. The difference in Ca^{2+} transient amplitude was not significant (*P*=0.082).

treatment, we measured global gene expression differences using RNA sequencing. There were 1133 genes differentially expressed in dSG KO versus WT hearts; treatment with the TPr antagonist normalized expression of 160 of these genes (Figure 8A and 8B). Via regulator pathway analysis, expression of dSG KO genes associated with cardiomyocyte survival were increased while cell death genes were decreased (Figure 8C) with TPr antagonism. Other gene changes include decreased expression of fibrosis and matrix-associated genes, and increased expression of genes associated with the cytoskeleton and fatty acid utilization (Figure 8D; complete data set is available at Gene Expression Omnibus, series accession GSE96598). Consistent with the increases seen in plasma atrial natriuretic peptide (Figure 3F), expression of the Nppa gene was increased 4.49-fold in dSG KO hearts versus WT hearts (*P*=1.24E-5), while ifetroban treatment of KO mice decreased Nppa 1.82-fold compared with vehicle (*P*=0.0038). Other genes were chosen to validate from RNAseq that belong to a core molecular signature of DMD, identified via integrative analysis of multiple mouse and human data sets.[42] Extracellular matrix–associated genes, including the matricellular protein lumican, are increased in mice and patients with MD.[42,43] dSG KO hearts have increased expression of Lum, which is reduced to WT levels in dSG mice given ifetroban (Figure 8E). We also confirmed a decrease in expression of the retinol-binding protein gene Rbp1 with TPr antagonism (Figure 8E), although we could not confirm the increase in expression seen in dSG KO mice by RNAseq (2.05-fold versus WT, *P*=8.68E-5). This likely reflects the moderating effects of pooling mRNAs for RNAseq replicates. Of note, however, we found that TPr antagonism significantly attenuated TPr gene expression in dSG mice (Tbxa2r; Figure 8E).

Discussion

In this study, we investigated the effects of long-term antagonism of the TPr on the development of fibrosis and

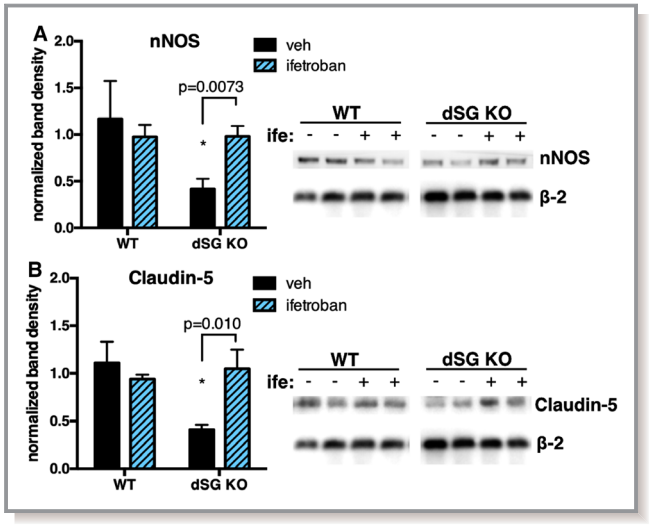

Figure 7. Expression of neuronal nitric oxide synthase (nNOS) and claudin-5 are improved in male δ-sarcoglycan (dSG) knockout (KO) hearts following thromboxane-prostanoid receptor antagonism. Shown are blots of total heart protein probed for nNOS (**A**) and claudin-5 (**B**), and the mean and standard error of ImageJ quantification using β2 microglobulin as loading control (n=5 per group pooled from 2 separate blots, with all groups included in each blot). The space between groups indicates missing lanes. Comparisons between vehicle- and drug-treated KO were made by 2-tailed *t* test and exact *P* values are shown; comparisons among groups were made by 2-way ANOVA (*$P<0.05$ from WT).

cardiomyopathy associated with MD. Treatment with the TPr antagonist ifetroban increased animal survival and improved the cardiac phenotype in 3 different murine models of MD. TPr antagonism improved cardiac output in 2 models of severe DMD, and increased ejection fraction while decreasing cardiac fibrosis, transforming growth factor-β signaling, and expression of matricellular genes in limb-girdle MD mice. DMD cardiomyopathy progresses from early fibrosis to diastolic dysfunction and eventual manifest systolic dysfunction.[44] Our data suggest that TPr antagonism delays both the systolic and diastolic dysfunction in mice, and this may prevent or delay clinical signs of cardiomyopathy in patients. The improvement in diastolic function results from decreased fibrosis as well as corrected Ca^{2+} decay and cardiomyocyte relaxation, while the improvement in systolic function is likely the result of improved loading conditions, cardiomyocyte preservation, and decreased fibrosis. Contraction deficits of individual cardiomyocytes were unchanged. Additionally, ifetroban increased expression of claudin-5 and nNOS protein, which have been shown to improve cardiac function in MD, and normalized expression of select genes typically upregulated in DMD. Altogether, these results suggest that the TPr is activated in MD and contributes to the cardiac phenotype.

The multiple genotypes used in our study likely model multiple mechanisms of cardiomyopathy,[45] as well as different aspects of the MD disease course, and partially reflect the heterogeneity of human MD. The mdx-based DMD mouse models, which lack dystrophin, had likely diastolic dysfunction (preserved ejection fraction but decreased cardiac output), while the dSG KO presented with systolic dysfunction as well as indices of diastolic dysfunction such as increased fibrosis and delayed cardiomyocyte relaxation. However, some cross-genotype comparisons in echocardiographic parameters may be inaccurate because our echocardiography was performed under isoflurane, the response to which could have disproportionately affected data from 1 set of mice. Because their severe kyphosis prevented intubation, it is unknown whether the DKO also had increased LV systolic pressure. Further experiments in a DMD cardiac mouse model with improved survival, such as the utrophin heterozygous mdx mice, will be critical to delineating the effect of TPr antagonism on diastolic function in these mice. Another caveat to this study is that our predetermined end point design did not allow for a complete survival analysis of the mice, and thus the exact survival benefits that TPr antagonism may confer are still unknown. Despite the predetermined end point, we cannot rule out a survivor effect on the DKO and mdx/mTR data, as well as on the data obtained from isolated dSG KO cardiomyocytes.

Expression and activation of the TPr is elevated during cardiovascular disease,[16,46,47] which also reduces the cardiac effects of antagonists in healthy controls.[16] While it can couple to $G_{12/13}$, and human isoforms may differentially affect cyclic AMP via G_i or G_s, the predominant described pathway for TPr signaling is via $G_{q/11}$ and phospholipase C.[17] This poises the receptor to have deleterious cardiovascular effects similar or complementary to other G_q-coupled receptors such as the angiotensin II or endothelin receptor in response to endogenous agonist.

The TPr is expressed in cardiomyocytes,[18] fibroblasts,[48] immune cells,[49,50] and vascular smooth muscle cells,[17] and it is likely that activation of the receptor on more than one of these cell types contributes to the pathology of MD. While beyond the scope of this study, a comprehensive analysis of TPr binding, localization, or ligand availability in healthy tissues compared with early or late MD would be illuminating. Here, we report an improvement in cardiac, but not skeletal muscle, fibrosis and function with TPr antagonism. This is likely the result of low receptor expression in skeletal muscle (Figure S2B), but could also reflect differential expression in resident fibroblast populations, or availability of endogenous ligand. We propose that the decreased cardiomyopathy seen in dSG KO mice after TPr antagonism is attributable to: (1) improved cardiomyocyte health, (2) decreased fibroblast proliferation and activation, and (3) subtle modulation of the immune response. It is difficult to say how much of (2) and (3) are dependent on (1), and vice versa. TPr activation in cardiomyocytes can cause

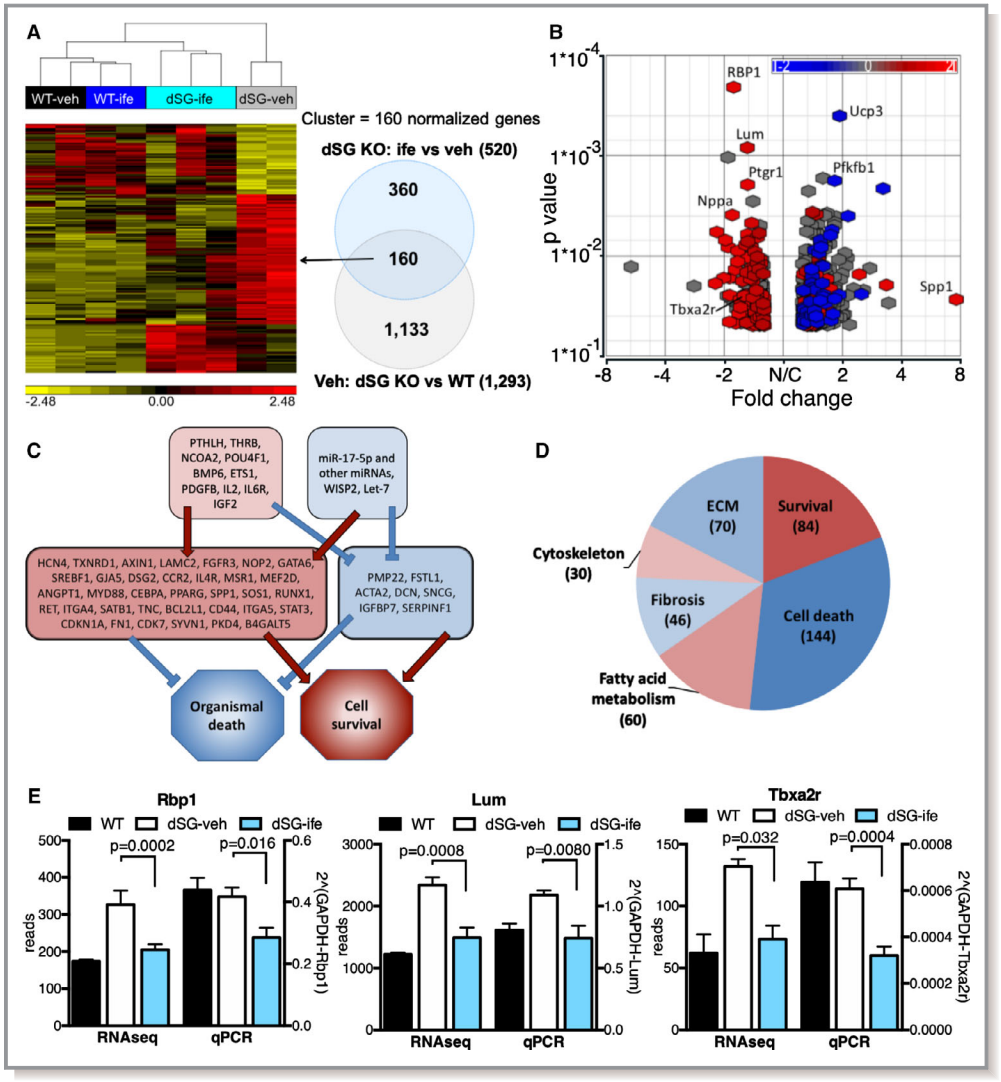

Figure 8. Changes in male cardiac gene expression with δ-sarcoglycan (dSG) knockout (KO) and thromboxane-prostanoid receptor (TPr) antagonism. **A**, A heat map of differentially expressed genes in RNAseq. 1133 genes were changed in KO vs wildtype (WT), while expression of 160 of these genes was normalized and 360 additional genes changed with ifetroban treatment. A volcano plot with detail of the overlapping genes is shown in (**B**), where expression changes with ifetroban treatment are plotted on the X axis, and changes resulting from dSG KO are indicated with red (+) or blue (−). **C**, Gene expression changes with TPr antagonism are predicted to increase cell survival and decrease organismal death. Comparing vehicle-treated and ifetroban-treated dSG KO, pathway analysis (Ingenuity, Qiagen) of differentially expressed genes (middle) predicted upstream (top) changes with the anticipated consequence of survival or organismal death (bottom). Blue indicates decreased and red with arrows indicates increased expression or activity. Major groups of significantly changed genes are shown in (**D**), where red indicates increased and blue indicates decreased expression. The total number of genes changed in each group is in parentheses, and was derived from Partek flow differential gene analysis. **E**, Reverse transcription polymerase chain reaction (qPCR) was used to confirm RNAseq results. Normalized RNAseq expression data are shown at left in each graph, compared with PCR results at right. Expression of the extracellular matrix (ECM) gene lumican is increased in muscular dystrophy and normalized with TPr antagonism, while expression of retinol-binding protein and TPr genes are reduced with TPr antagonism. Comparisons of vehicle- and drug-treated qPCR are by 2-tailed *t* test; the mean and standard error are shown. n=5 for PCR and n=2 sample pools per group for RNAseq except dSG-ifetroban n=3.

intracellular calcium transients, increased free intracellular calcium, and arrhythmia in both isolated beating cells and whole animals,[19,51] which may increase the chance of cellular death[52] or sudden cardiac death. This may be one explanation for the improved survival and reduced sudden death following TPr antagonism in DKO mice, a model of

DMD that had not yet developed cardiac fibrosis at the time of euthanization. Future studies with isoproterenol challenge can directly determine whether TPr antagonism is protective against induced arrhythmia and sudden cardiac death. MD cardiomyocytes are particularly susceptible to arrhythmia and sensitive to Ca^{2+} overload, which can activate Ca^{2+}-sensitive proteases and lead to cell death.[53] In this study, we saw delayed Ca^{2+} clearance and relaxation in isolated dSG KO cardiomyocytes. These changes were ameliorated in ifetroban-treated dSG KO cardiomyocytes, one means by which TPr antagonism could improve diastolic dysfunction in MD. However, we did not see an increase in resting (end-diastolic) Ca^{2+} in dSG KO cardiomyocytes, suggesting that the isolated cells healthy enough for experimentation did not have Ca^{2+} overload. Because these experiments were designed to investigate long-term cardiomyocyte effects of dSG KO genotype or drug treatment, further cardiomyocyte experiments in the presence of agonist and/or antagonist will be informative.

Besides decreased reaction attributable to improved cardiomyocyte health, it is possible for fibroblasts and immune cells to be directly affected by TPr antagonism.[49,50] TPr activation is generally stimulatory and induces lymphocyte[50,54] and fibroblast proliferation and collagen production.[48] We found that hearts from dSG KO mice treated with a TPr antagonist expressed lower levels of fibrosis and matrix-associated genes. There were also multiple changed genes relating to immune function (see table of group comparison statistics in Data S1), and male dSG KO mice had increased circulating total white blood cells and lymphocytes (Table S1), which was normalized with TPr antagonism. Therefore, the decrease in Tbxa2r expression that we detected by RNAseq and polymerase chain reaction in ifetroban-treated dSG KO mice could also reflect a decreased population of immune cells or fibroblasts that are high-expressing.

In addition, the TPr is well-described in smooth muscle cells, and its activation causes vasoconstriction, proliferation, and coronary dysfunction.[17,55] Because the dSG KO mouse is associated with coronary dysfunction,[25] prevention of vasoconstriction may be one means by which TPr antagonism may improve dSG KO cardiac function. We did find that the vehicle-treated, but not ifetroban-treated, dSG KO mice had noticeably increased LV systolic pressure. This could indicate inhibition of TPr-mediated vasoconstriction or vascular remodeling, but it is also possible that long-term blockade of TPr activation either reduces sympathetic tone or modulates its effects on the heart, as endogenous TPr activation contributes to angiotensin II–dependent hypertension and cardiac damage.[11] Further experiments using telemetry and pressure-volume catheterization will be needed to determine the effect of TPr antagonism on systemic vascular resistance in DMD mouse models. There is evidence that individuals with DMD may have increased arterial stiffness even with normal systemic pressure,[56] and reports suggest that early treatment to maintain normal vascular resistance is beneficial in MD.[57]

The contribution of the TPr to multiple causes in MD is likely reflected in the murine survival benefits of antagonism. Some animals in our study died unexpectedly from likely cardiac causes, while others declined in weight before death despite in-cage supplementation. A subset of vehicle-treated DKO mice that were accidentally placed on high-calorie breeder chow for several weeks had 100% survival (Figure 1 and the Table), and 1 vehicle-treated dSG KO mouse had gross dilatation of the colon at euthanization (Figure S3). Gastrointestinal deficits are well-described in DMD[58] and, although there was no overall effect of antagonism on DKO weight (Table), it is possible that blockade of TPr activity in intestinal smooth muscle improved intestinal function and overall nutrition. It is also possible that modulation of the immune response in TPr blockade, combined with the propensity of MD mice to poor airway clearance and respiratory failure, prevented some deaths. Finally, increased nNOS expression could also contribute to survival by decreasing oxidative stress. Future studies are necessary to further define the TPr contribution to MD pathology and mortality, and MD mouse models will need to be crossed with cell-specific TPr KO to more specifically determine individual contributions.

Conclusions

The TPr is activated by multiple endogenous ligands, including thromboxane A_2, 20-hydroxyeicosatetraenoic acid, and F_{2t}-isoprostane, and, thus, in systems where the principal ligand is not thromboxane, the effects of a TPr antagonist cannot be duplicated by cyclooxygenase or thromboxane synthase inhibitors. Our results suggest that decreasing endogenous activation of the TPr may ameliorate some consequences of dystrophin-associated protein complex disruption in cardiomyocytes, and that oral TPr antagonists may be a novel therapeutic to improve the cardiac phenotype and decrease mortality in MD.

Acknowledgments

The authors would like to thank Dr Kevin Campbell, University of Iowa, for his generous gift of the dSG KO mice.

Sources of Funding

This project was funded by Cumberland Pharmaceuticals Inc and the Fight DMD Foundation, as well as by National Institutes of Health P01 HL 108800 and R01 HL 135011. Cumberland Pharmaceuticals Inc, which partially funded this

project, owns ifetroban through Cumberland Emerging Technologies, a joint initiative between Cumberland Pharmaceuticals, Vanderbilt University, and the Tennessee Technology Development Corporation.

Disclosures

None.

References

1. Emery AE. Population frequencies of inherited neuromuscular diseases—a world survey. *Neuromuscul Disord*. 1991;1:19–29.
2. Burr AR, Molkentin JD. Genetic evidence in the mouse solidifies the calcium hypothesis of myofiber death in muscular dystrophy. *Cell Death Differ*. 2015;22:1402–1412.
3. Finsterer J, Cripe L. Treatment of dystrophin cardiomyopathies. *Nat Rev Cardiol*. 2014;11:168–179.
4. Ho R, Nguyen ML, Mather P. Cardiomyopathy in Becker muscular dystrophy: overview. *World J Cardiol*. 2016;8:356–361.
5. Hermans MC, Pinto YM, Merkies IS, de Die-Smulders CE, Crijns HJ, Faber CG. Hereditary muscular dystrophies and the heart. *Neuromuscul Disord*. 2010;20:479–492.
6. Frankel KA, Rosser RJ. The pathology of the heart in progressive muscular dystrophy: epimyocardial fibrosis. *Hum Pathol*. 1976;7:375–386.
7. Menon SC, Etheridge SP, Liesemer KN, Williams RV, Bardsley T, Heywood MC, Puchalski MD. Predictive value of myocardial delayed enhancement in Duchenne muscular dystrophy. *Pediatr Cardiol*. 2014;35:1279–1285.
8. Verhaert D, Richards K, Rafael-Fortney JA, Raman SV. Cardiac involvement in patients with muscular dystrophies: magnetic resonance imaging phenotype and genotypic considerations. *Circ Cardiovasc Imaging*. 2011;4:67–76.
9. James J, Kinnett K, Wang Y, Ittenbach RF, Benson DW, Cripe L. Electrocardiographic abnormalities in very young Duchenne muscular dystrophy patients precede the onset of cardiac dysfunction. *Neuromuscul Disord*. 2011;21:462–467.
10. Rajdev A, Groh WJ. Arrhythmias in the muscular dystrophies. *Card Electrophysiol Clin*. 2015;7:303–308.
11. Francois H, Athirakul K, Mao L, Rockman H, Coffman TM. Role for thromboxane receptors in angiotensin-II-induced hypertension. *Hypertension*. 2004;43:364–369.
12. Francois H, Makhanova N, Ruiz P, Ellison J, Mao L, Rockman HA, Coffman TM. A role for the thromboxane receptor in L-NAME hypertension. *Am J Physiol Renal Physiol*. 2008;295:F1096–F1102.
13. Zhang Z, Vezza R, Plappert T, McNamara P, Lawson JA, Austin S, Pratico D, St-John Sutton M, FitzGerald GA. COX-2-dependent cardiac failure in Gh/tTG transgenic mice. *Circ Res*. 2003;92:1153–1161.
14. Acquaviva A, Vecchio D, Arezzini B, Comporti M, Gardi C. Signaling pathways involved in isoprostane-mediated fibrogenic effects in rat hepatic stellate cells. *Free Radic Biol Med*. 2013;65:201–207.
15. Gelosa P, Sevin G, Pignieri A, Budelli S, Castiglioni L, Blanc-Guillemaud V, Lerond L, Tremoli E, Sironi L. Terutroban, a thromboxane/prostaglandin endoperoxide receptor antagonist, prevents hypertensive vascular hypertrophy and fibrosis. *Am J Physiol Heart Circ Physiol*. 2011;300:H762–H768.
16. West JD, Voss BM, Pavliv L, de Caestecker M, Hemnes AR, Carrier EJ. Antagonism of the thromboxane-prostanoid receptor is cardioprotective against right ventricular pressure overload. *Pulm Circ*. 2016;6:211–223.
17. Huang JS, Ramamurthy SK, Lin X, Le Breton GC. Cell signalling through thromboxane A2 receptors. *Cell Signal*. 2004;16:521–533.
18. Wacker MJ, Kosloski LM, Gilbert WJ, Touchberry CD, Moore DS, Kelly JK, Brotto M, Orr JA. Inhibition of thromboxane A2-induced arrhythmias and intracellular calcium changes in cardiac myocytes by blockade of the inositol trisphosphate pathway. *J Pharmacol Exp Ther*. 2009;331:917–924.
19. Wacker MJ, Best SR, Kosloski LM, Stachura CJ, Smoot RL, Porter CB, Orr JA. Thromboxane A2-induced arrhythmias in the anesthetized rabbit. *Am J Physiol Heart Circ Physiol*. 2006;290:H1353–H1361.
20. Grosso S, Perrone S, Longini M, Bruno C, Minetti C, Gazzolo D, Balestri P, Buonocore G. Isoprostanes in dystrophinopathy: evidence of increased oxidative stress. *Brain Dev*. 2008;30:391–395.
21. Cracowski JL, Tremel F, Marpeau C, Baguet JP, Stanke-Labesque F, Mallion JM, Bessard G. Increased formation of F(2)-isoprostanes in patients with severe heart failure. *Heart*. 2000;84:439–440.
22. Deconinck AE, Rafael JA, Skinner JA, Brown SC, Potter AC, Metzinger L, Watt DJ, Dickson JG, Tinsley JM, Davies KE. Utrophin-dystrophin-deficient mice as a model for Duchenne muscular dystrophy. *Cell*. 1997;90:717–727.
23. Sacco A, Mourkioti F, Tran R, Choi J, Llewellyn M, Kraft P, Shkreli M, Delp S, Pomerantz JH, Artandi SE, Blau HM. Short telomeres and stem cell exhaustion model Duchenne muscular dystrophy in mdx/mTR mice. *Cell*. 2010;143:1059–1071.
24. Mourkioti F, Kustan J, Kraft P, Day JW, Zhao MM, Kost-Alimova M, Protopopov A, DePinho RA, Bernstein D, Meeker AK, Blau HM. Role of telomere dysfunction in cardiac failure in Duchenne muscular dystrophy. *Nat Cell Biol*. 2013;15:895–904.
25. Coral-Vazquez R, Cohn RD, Moore SA, Hill JA, Weiss RM, Davisson RL, Straub V, Barresi R, Bansal D, Hrstka RF, Williamson R, Campbell KP. Disruption of the sarcoglycan-sarcospan complex in vascular smooth muscle: a novel mechanism for cardiomyopathy and muscular dystrophy. *Cell*. 1999;98:465–474.
26. McDonald AA, Hebert SL, Kunz MD, Ralles SJ, McLoon LK. Disease course in mdx:utrophin$^{+/-}$ mice: comparison of three mouse models of Duchenne muscular dystrophy. *Physiol Rep*. 2015;3:e12391.
27. van Putten M, Kumar D, Hulsker M, Hoogaars WM, Plomp JJ, van Opstal A, van Iterson M, Admiraal P, van Ommen GJ, 't Hoen PA, Aartsma-Rus A. Comparison of skeletal muscle pathology and motor function of dystrophin and utrophin deficient mouse strains. *Neuromuscul Disord*. 2012;22:406–417.
28. van Putten M. The use of hanging wire tests to monitor muscle strength and condition over time. *DMD_M.2.1.004*. 2011.
29. Hemnes AR, Maynard KB, Champion HC, Gleaves L, Penner N, West J, Newman JH. Testosterone negatively regulates right ventricular load stress responses in mice. *Pulm Circ*. 2012;2:352–358.
30. Rüegg MA, Meinen S. Histopathology in Masson Trichrome stained muscle sections. *MDCIA_M.1.2.003*. 2011.
31. Knollmann BC, Chopra N, Hlaing T, Akin B, Yang T, Ettensohn K, Knollmann BE, Horton KD, Weissman NJ, Holinstat I, Zhang W, Roden DM, Jones LR, Franzini-Armstrong C, Pfeifer K. Casq2 deletion causes sarcoplasmic reticulum volume increase, premature Ca^{2+} release, and catecholaminergic polymorphic ventricular tachycardia. *J Clin Invest*. 2006;116:2510–2520.
32. Roth GM, Bader DM, Pfaltzgraff ER. Isolation and physiological analysis of mouse cardiomyocytes. *J Vis Exp*. 2014;(91):e51109.
33. Pasteuning-Vuhman S, Putker K, Tanganyika-de Winter CL, Boertje-van der Meulen JW, van Vliet L, Overzier M, Plomp JJ, Aartsma-Rus A, van Putten M. Natural disease history of mouse models for limb girdle muscular dystrophy types 2D and 2F. *PLoS One*. 2017;12:e0182704.
34. Bia BL, Cassidy PJ, Young ME, Rafael JA, Leighton B, Davies KE, Radda GK, Clarke K. Decreased myocardial nNOS, increased iNOS and abnormal ECGs in mouse models of Duchenne muscular dystrophy. *J Mol Cell Cardiol*. 1999;31:1857–1862.
35. Tidball JG, Wehling-Henricks M. Nitric oxide synthase deficiency and the pathophysiology of muscular dystrophy. *J Physiol*. 2014;592:4627–4638.
36. Lai Y, Zhao J, Yue Y, Wasala NB, Duan D. Partial restoration of cardiac function with DeltaPDZ nNOS in aged mdx model of Duchenne cardiomyopathy. *Hum Mol Genet*. 2014;23:3189–3199.
37. Wehling-Henricks M, Jordan MC, Roos KP, Deng B, Tidball JG. Cardiomyopathy in dystrophin-deficient hearts is prevented by expression of a neuronal nitric oxide synthase transgene in the myocardium. *Hum Mol Genet*. 2005;14:1921–1933.
38. Milani-Nejad N, Schultz EJ, Slabaugh JL, Janssen PM, Rafael-Fortney JA. Myocardial contractile dysfunction is present without histopathology in a mouse model of limb-girdle muscular dystrophy-2F and is prevented after claudin-5 virotherapy. *Front Physiol*. 2016;7:539.
39. Sanford JL, Edwards JD, Mays TA, Gong B, Merriam AP, Rafael-Fortney JA. Claudin-5 localizes to the lateral membranes of cardiomyocytes and is altered in utrophin/dystrophin-deficient cardiomyopathic mice. *J Mol Cell Cardiol*. 2005;38:323–332.
40. Mays TA, Binkley PF, Lesinski A, Doshi AA, Quaile MP, Margulies KB, Janssen PM, Rafael-Fortney JA. Claudin-5 levels are reduced in human end-stage cardiomyopathy. *J Mol Cell Cardiol*. 2008;45:81–87.
41. Delfín DA, Xu Y, Schill KE, Mays TA, Canan BD, Zang KE, Barnum JA, Janssen PM, Rafael-Fortney JA. Sustaining cardiac claudin-5 levels prevents functional hallmarks of cardiomyopathy in a muscular dystrophy mouse model. *Mol Ther*. 2012;20:1378–1383.

42. Ichim-Moreno N, Aranda M, Voolstra CR. Identification of a gene expression core signature for Duchenne muscular dystrophy (DMD) via integrative analysis reveals novel potential compounds for treatment. *2010 IEEE Symposium on Computational Intelligence in Bioinformatics and Computational Biology*. 2010:1–6.
43. Pescatori M, Broccolini A, Minetti C, Bertini E, Bruno C, D'Amico A, Bernardini C, Mirabella M, Silvestri G, Giglio V, Modoni A, Pedemonte M, Tasca G, Galluzzi G, Mercuri E, Tonali PA, Ricci E. Gene expression profiling in the early phases of DMD: a constant molecular signature characterizes DMD muscle from early postnatal life throughout disease progression. *FASEB J*. 2007;21:1210–1226.
44. Markham LW, Michelfelder EC, Border WL, Khoury PR, Spicer RL, Wong BL, Benson DW, Cripe LH. Abnormalities of diastolic function precede dilated cardiomyopathy associated with Duchenne muscular dystrophy. *J Am Soc Echocardiogr*. 2006;19:865–871.
45. Townsend D, Yasuda S, McNally E, Metzger JM. Distinct pathophysiological mechanisms of cardiomyopathy in hearts lacking dystrophin or the sarcoglycan complex. *FASEB J*. 2011;25:3106–3114.
46. Katugampola SD, Davenport AP. Thromboxane receptor density is increased in human cardiovascular disease with evidence for inhibition at therapeutic concentrations by the AT1 receptor antagonist losartan. *Br J Pharmacol*. 2001;134:1385–1392.
47. Smyth EM. Thromboxane and the thromboxane receptor in cardiovascular disease. *Clin Lipidol*. 2010;5:209–219.
48. Arezzini B, Vecchio D, Signorini C, Stringa B, Gardi C. F2-isoprostanes can mediate bleomycin-induced lung fibrosis. *Free Radic Biol Med*. 2018;115:1–9.
49. Hartney JM, Gustafson CE, Bowler RP, Pelanda R, Torres RM. Thromboxane receptor signaling is required for fibronectin-induced matrix metalloproteinase 9 production by human and murine macrophages and is attenuated by the Arhgef1 molecule. *J Biol Chem*. 2011;286:44521–44531.
50. Ushikubi F, Aiba Y, Nakamura K, Namba T, Hirata M, Mazda O, Katsura Y, Narumiya S. Thromboxane A2 receptor is highly expressed in mouse immature thymocytes and mediates DNA fragmentation and apoptosis. *J Exp Med*. 1993;178:1825–1830.
51. Hoffmann P, Heinroth-Hoffmann I, Toraason M. Alterations by a thromboxane A2 analog (U46619) of calcium dynamics in isolated rat cardiomyocytes. *J Pharmacol Exp Ther*. 1993;264:336–344.
52. Touchberry CD, Silswal N, Tchikrizov V, Elmore CJ, Srinivas S, Akthar AS, Swan HK, Wetmore LA, Wacker MJ. Cardiac thromboxane A2 receptor activation does not directly induce cardiomyocyte hypertrophy but does cause cell death that is prevented with gentamicin and 2-APB. *BMC Pharmacol Toxicol*. 2014;15:73.
53. Ameen V, Robson LG. Experimental models of Duchenne muscular dystrophy: relationship with cardiovascular disease. *Open Cardiovasc Med J*. 2010;4:265–277.
54. Thomas DW, Rocha PN, Nataraj C, Robinson LA, Spurney RF, Koller BH, Coffman TM. Proinflammatory actions of thromboxane receptors to enhance cellular immune responses. *J Immunol*. 2003;171:6389–6395.
55. Gupte SA, Okada T, Tateyama M, Ochi R. Activation of TxA2/PGH2 receptors and protein kinase C contribute to coronary dysfunction in superoxide treated rat hearts. *J Mol Cell Cardiol*. 2000;32:937–946.
56. Ryan TD, Parent JJ, Gao Z, Khoury PR, Dupont E, Smith JN, Wong B, Urbina EM, Jefferies JL. Central arterial function measured by non-invasive pulse wave analysis is abnormal in patients with Duchenne muscular dystrophy. *Pediatr Cardiol*. 2017;38:1269–1276.
57. van de Velde NM, Roest AAW, van Zwet EW, Niks EH. Increased blood pressure and body mass index as potential modifiable factors in the progression of myocardial dysfunction in Duchenne muscular dystrophy. *J Neuromuscul Dis*. 2019;6:65–73.
58. Lo Cascio CM, Goetze O, Latshang TD, Bluemel S, Frauenfelder T, Bloch KE. Gastrointestinal dysfunction in patients with Duchenne muscular dystrophy. *PLoS One*. 2016;11:e0163779.

SUPPLEMENTAL MATERIAL

Data S1. Supplementary Methods

RNAseq analysis

RNA was pooled from 1-3 individual mice, depending on quality and integrity of available RNA, for a total of 300 ng. Pools primarily consisted of littermates, and an equal amount of RNA from each sample was added. cDNA Library preparation was accomplished using the Illumina TruSeq stranded mRNA Sample Preparation Kit and samples sequenced on the Illumina HiSeq 2500 on 75 bp paired-end runs at 30 million passing filter reads/sample. RNA sequencing analysis was performed using Partek Flow software (Build version 7.0.18.0820) and core processors (Partek, Inc. St. Louis, MO) in conjunction with the following external tools: java 1.8.0_181, perl v5.2.1, Python 2.7.12, pip 18.0, and R version 3.4.4. Raw reads (fastq files) were aligned to the *Mus musculus* genome (reference mm10) using STAR version 2.5.3a. Based on post-alignment quality assurance and control (QA/QC), all samples were of high fidelity; i.e., Phred quality score = 38.98 ± 0.48, indicating a high probability that the bases were accurately identified. The Phred score = -10*log10(Probability of Error). Aligned reads were normalized to total reads per sample, followed by quantification using P/E (Partek's optimization of the expectation-maximization algorithm) [1] and then log-transformed with offset of 0.0001, with statistical comparison of groups using Partek's best fit multimodel algorithm GSA (Gene Specific Analysis) with the following default parameters: AICc model selection, lognormal with shrinkage distribution with F statistics and FDR step-up. PCA (with correlation matrix) and hierarchical clustering (with Euclidian distance and Average linkage) were performed using Partek Genomics Suite 6.6.

Functional Analysis

Individual gene functions, as presented in significant gene list tables, were determined using publicly available records using NCBI Entrez Gene, Aceview, and Pubmed databases. Statistical analyses (including correction for multiple hypothesis testing) for identification of overrepresented ontologies, functions, and pathways were performed using DAVID [2, 3], a freely available online-based functional analysis tool (http://david.abcc.ncifcrf.gov), after initial statistical data analysis was performed to identify relevant gene sets. AmiGO was used for functional grouping of genes, with reported results limited to those ontologies identified as significantly enriched using Panther and DAVID. Gene Set Enrichment Analysis (GSEA), available online through the BROAD Institute [4, 5], was also used to evaluate biological process enrichment and to identify activation of transcription factors based on locations of their conserved motifs in or near significantly altered genes. Ingenuity Pathway Analysis (Qiagen) was used for Upstream Regulator Analysis, which predicts upstream signaling molecules that could be responsible for the observed gene expression changes between WT and dSG KO mice.

References Cited

1. Li B, Ruotti V, Stewart RM, Thomson JA, Dewey CN. Rna-seq gene expression estimation with read mapping uncertainty. *Bioinformatics*. 2010;26:493-500

2. Huang DW, Sherman BT, Lempicki RA. Systematic and integrative analysis of large gene lists using david bioinformatics resources. *Nat. Protoc.* 2009;4:44-57

3. Huang DW, Sherman BT, Lempicki RA. Bioinformatics enrichment tools: Paths toward the comprehensive functional analysis of large gene lists. *Nucleic Acids Res.* 2009;37:1-13

4. Mootha VK, Lindgren CM, Eriksson KF, Subramanian A, Sihag S, Lehar J, Puigserver P, Carlsson E, Ridderstrale M, Laurila E, Houstis N, Daly MJ, Patterson N, Mesirov JP, Golub TR, Tamayo P, Spiegelman B, Lander ES, Hirschhorn JN, Altshuler D, Groop LC. Pgc-1 alpha-

responsive genes involved in oxidative phosphorylation are coordinately downregulated in human diabetes. *Nat. Genet.* 2003;34:267-273

5. Subramanian A, Tamayo P, Mootha VK, Mukherjee S, Ebert BL, Gillette MA, Paulovich A, Pomeroy SL, Golub TR, Lander ES, Mesirov JP. Gene set enrichment analysis: A knowledge-based approach for interpreting genome-wide expression profiles. *Proc. Natl. Acad. Sci. U. S. A.* 2005;102:15545-15550

Table S1: Complete blood count of ∂-sarcoglycan (dSG) knockout mice.

	WBC (10^3 cells/μL)	Neutrophils (10^3 cells/μL)	Lymphocytes (10^3 cells/μL)	Monocytes (10^3 cells/μL)	RBC (10^6 cells/μL)	n
Wildtype	8.14 ± 2.65	1.42 ± 0.48	6.40 ± 2.17	0.31 ± 0.14	9.77 ± 0.08	5
dSG-vehicle	12.44 ± 1.34 *p=0.022 vs WT	2.16 ± 0.39 *p=0.045 vs WT	9.94 ± 1.06 *p=0.021 vs WT	0.34 ± 0.11	9.48 ± 0.16	4
dSG-ifetroban	9.10 ± 2.52 p=0.053 vs veh	1.74 ± 0.49 p=0.24 vs veh	6.80 ± 2.18 *p=0.041 vs veh	0.27 ± 0.15	9.80 ± 0.64	4

Table S1: Mean ± standard deviation of a complete blood count taken from male mice at sacrifice. Comparisons are by unpaired two-tailed t-test.

Figure S1

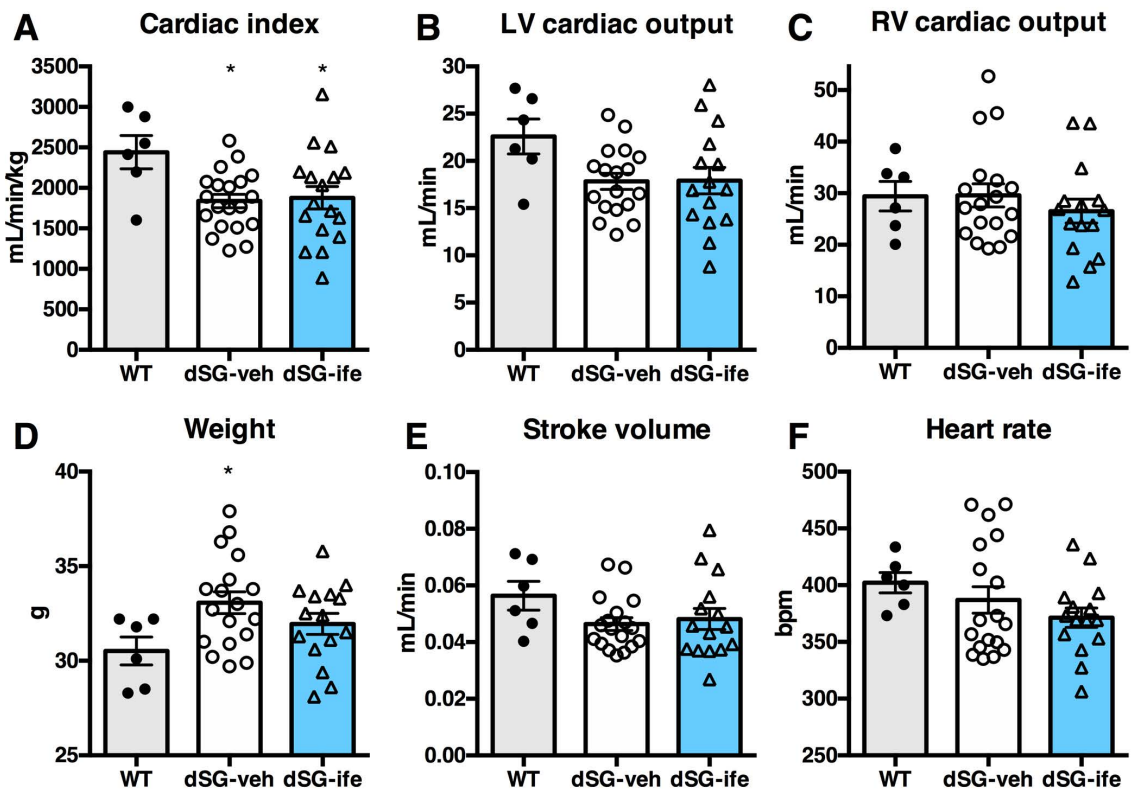

Figure S1: Weight changes contribute to the cardiac index (CI). Both groups of male ∂-sarcoglycan (dSG) knockout (KO) mice have a decreased left ventricular (LV) cardiac index compared with male wildtype (WT), as measured by echocardiography (**A**). However, the difference in actual LV cardiac output does not significantly differ from WT (p=0.093 for each group) because the hind leg pseudohypertrophy of dSG KO contributes to an elevated body weight (**B and D**). RV cardiac output is also unchanged (**C**) LV cardiac output is calculated by (stroke volume)*(heart rate) and the distribution of these metrics is also shown from the mice who underwent successful echocardiography (**E-F**). No vehicle and ifetroban-treated KO groups were significantly different by two-tailed t test. Error bars reflect SEM of the mean; *, p<0.05 from WT by one-way ANOVA followed by Holm-Sidak.

Figure S2

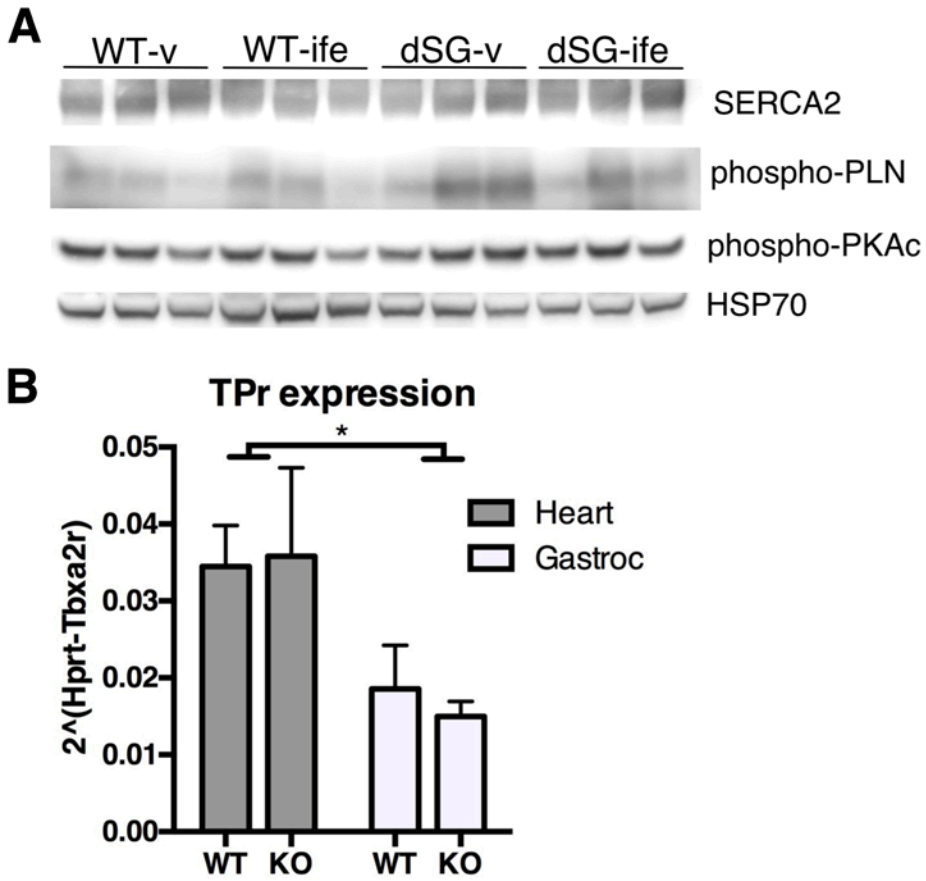

Figure S2: A) There is no decrease of SERCA2 protein or phospho-phospholamban (phospho-PLN) levels in ∂-sarcoglycan (dSG) knockout (KO) mouse heart. Shown are results of western blotting for SERCA2, phospho-PLN, and phospho-protein kinase A catalytic subunit (phospho-PKAc), alongside the western blot for heat shock protein 70 (HSP70) as loading control. **B**) TPr expression is greater in dSG KO heart compared with gastrocnemius skeletal muscle. RT-PCR for TPr (Tbxa2r) in wildtype and dSG KO mouse heart and gastrocnemius (n=4); heart and gastrocnemius were taken from the same mice. *, p=0.022 by two-way ANOVA.

Figure S3

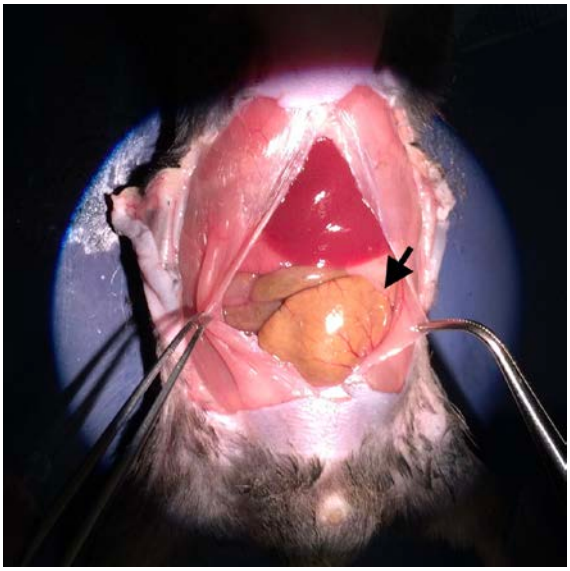

Figure S3: A vehicle-treated ∂-sarcoglycan knockout mouse with distended colon (arrow). Incidentally found at sacrifice, at 6 months of age.